PII S0016-7037(00)00886-9

Remobilization of authigenic uranium in marine sediments by bioturbation

YAN ZHENG,[1,2,]* ROBERT F. ANDERSON,[1,2] ALEXANDER VAN GEEN,[1] and MARTIN Q. FLEISHER[1]

[1]Lamont-Doherty Earth Observatory of Columbia University, New York, NY 10964, USA
[2]Department of Earth and Environmental Sciences, Columbia University, New York, NY 10964, USA

Abstract—Uranium behaves as a nearly conservative element in oxygenated seawater, but it is precipitated under chemically reducing conditions that occur in sediments underlying low-oxygen bottom water or in sediments receiving high fluxes of particulate organic carbon. Sites characterized by a range of bottom-water oxygen (BWO) and organic carbon flux (OCF) were studied to better understand the conditions that determine formation and preservation of authigenic U in marine sediments. Our study areas are located in the mid latitudes of the northeast Pacific and the northwest Atlantic Oceans, and all sites receive moderate (0.5 g/cm^2 kyr) to high (2.8 g/cm^2 kyr) OCF to the sediments. BWO concentrations vary substantially among the sites, ranging from <3 to ~270 μM. A mass balance approach was used to evaluate authigenic U remobilization at each site. Within each region studied, the supply of particulate nonlithogenic U associated with sinking particles was evaluated by means of sediment traps. The diffusive flux of U into sediments was calculated from pore-water U concentration profiles. These combined sources were compared with the burial rate of authigenic U to assess the efficiency of its preservation. A large fraction (one-third to two-thirds) of the authigenic U precipitated in these sediments via diffusion supply is later regenerated, even under very low BWO concentrations (~15 μM). Bioturbating organisms periodically mix authigenic U-containing sediment upward toward the sediment–water interface, where more oxidizing conditions lead to the remobilization of authigenic U and its loss to bottom waters. *Copyright © 2002 Elsevier Science Ltd*

1. INTRODUCTION

Over the past 20 years, much progress has been made in the understanding of the marine geochemistry of U, particularly regarding the pathways of removal from the ocean via precipitation in chemically reducing sediments. Pore-water depletion of U and sediment enrichment of U over detrital background levels by 1 to 10 μg/g have been observed in a number of anoxic basins (Anderson, 1987; Huh et al., 1987; Francois, 1988; Anderson et al., 1989b), as well as in hemipelagic sediments (Fleisher et al., 1986; Wallace et al., 1988; Barnes and Cochran, 1990; Klinkhammer and Palmer, 1991; Sirocko et al., 1991; Nameroff, 1996). Diffusion of U(VI) from bottom water into sediments, followed by reduction to U(IV), which is precipitated or adsorbed to sediment solids, is regarded as the primary source of authigenic U in these sediments. There is no doubt that authigenic U formation in suboxic and anoxic sediments is the most important mechanism removing U from ocean water, accounting for 40 to 70% of the riverine U input flux (Fleisher et al., 1986; Barnes and Cochran, 1990; Klinkhammer and Palmer, 1991).

Despite this general understanding, fundamental questions concerning the processes removing U from the oceans remain unanswered. In particular, the efficiency with which authigenic U, once formed, is preserved and buried has never been evaluated, nor have factors affecting authigenic U preservation been assessed. The accumulation rate of authigenic U in sediments reflects not only the input from diffusion and sinking particulate matter, but also the loss caused by U regeneration.

Both particulate nonlithogenic U (PNU) formed in surface waters and sediment authigenic U precipitated in situ are subject to remobilization when sediments are exposed to oxygen (Cochran et al., 1986; Zheng et al., 2002). Bioirrigation also oxygenates sediment (Martin and Sayles, 1987). Bioturbation stirs reducing sediment containing authigenic U up toward the sediment–water interface. In both cases, exposure to more oxidizing conditions may result in the release of U back to the water column.

In this study, we address the preservation efficiency of authigenic U in marine sediments through pore-water and sediment studies from a number of natural environments. These sites are selected because they represent a wide range of bottom-water oxygen (BWO) and a reasonable range of organic carbon flux (OCF) boundary conditions. Our sites are from the eastern and western continental margins of the United States, in the mid latitudes of the northeast Pacific and the northwest Atlantic Oceans (Fig. 1). The strategy is to construct a mass budget for U at each site whereby the flux of regenerated U can be estimated from the difference between the measured sources (the sinking flux of PNU together with the in situ precipitation of authigenic U supplied via diffusion through pore waters) and the measured long-term accumulation rate of authigenic U. The objective is to determine how each process affecting the accumulation rate of authigenic U changes in response to varying environmental boundary conditions.

2. GEOCHEMICAL SETTINGS OF THE STUDY SITES

The southern California Borderland includes the continental margin between Point Conception, California, and Viscaino Bay, Baja California. It consists of a network of submarine ridges, sills, and islands (Emery, 1960). The position of the sill depths with respect to the oxygen minimum zone of the north
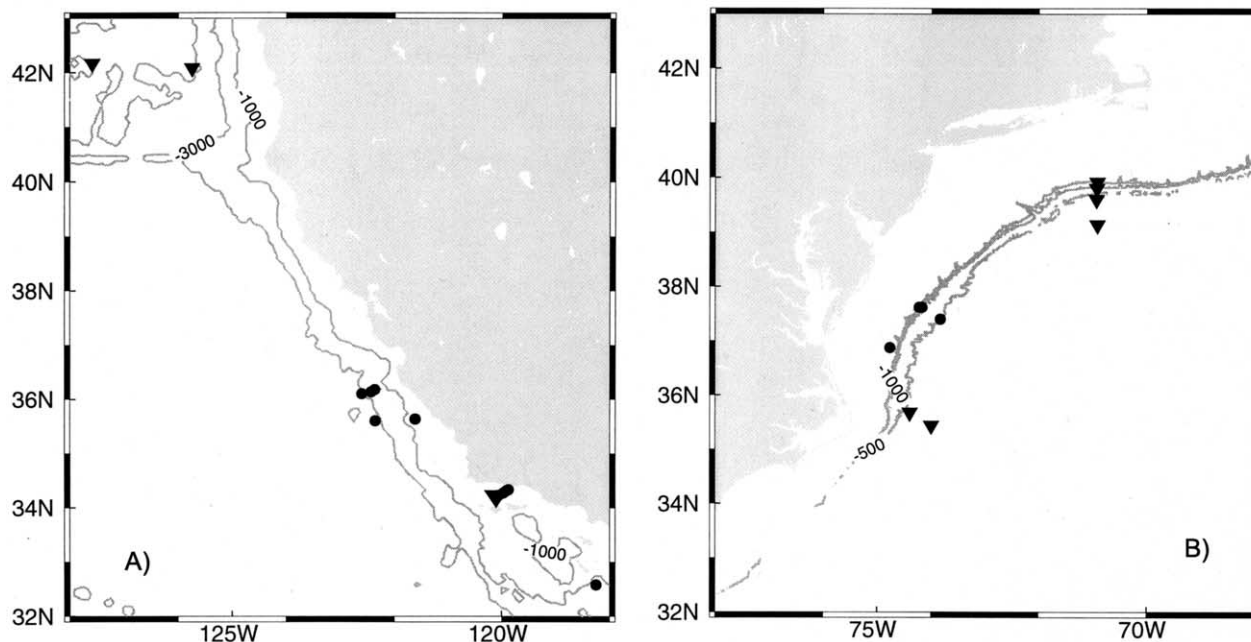

Fig. 1. (A) Locations of cores in the SBB, in the SCB, and along the California Margin (solid circles). Locations of sediment traps deployed during the MULTITRACER program (Lyle et al., 1992, at ~42°N, excluding the Gyre site) are also indicated (inverted triangles). The location of the sediment trap deployed in the SBB by Thunell et al. (1995) is also indicated by an inverted triangle. The bathymetry contours are 1000 and 3000 m. (B) Locations of cores in the MAB SEEP-II region (solid circles), as well as the locations of sediment traps deployed at the SEEP-I region (~39.5°N) and the SYNOP region (~35.5°N) (inverted triangles). The bathymetry contours are 500, 1000, and 2000 m, respectively. The source of bathymetry data is the HYDNOS data set from NOAA, which is a compilation of high-resolution U.S. coastal bathymetry.

Pacific Ocean and consumption of BWO during circulation through the basin result in BWO concentrations that vary from basin to basin (Sholkovitz and Gieskes, 1971; Shaw et al., 1990). Compared with Santa Barbara Basin (SBB), with a sill depth of 475 m and a BWO concentration ranging from <3 to 25 μM (Fig. 2A), San Clemente Basin (SCB) has a deeper sill depth of ~1800 m and a higher BWO concentration of 57 μM (Fig. 2B). In addition, the OCF in the SBB is 2.8 g/cm^2 kyr (Thunell et al., 1995) and is only 0.8 g/cm^2 kyr in the SCB (Jahnke, 1990). The sediment accumulation rate is ~50 to 100 g/cm^2 kyr in the SBB (Bruland et al., 1981), and only 5 to 15 g/cm^2 kyr in the SCB (Jahnke, 1990).

Along the continental slope of the northern California Margin, BWO concentrations range from ~12 μM in the oxygen minimum zone (~800 m, σ_θ = 27.2) to ~140 μM below ~3500 m (Fig. 1). The OCF is ~0.5 g/cm^2 kyr at ~42°N at a near shore site (<100 km offshore; Lyle et al., 1992). Sediment accumulates at a rate of 1 to 10 g/cm^2 kyr at sites near 35°N (Reimers et al., 1992; Gardner et al., 1997).

The Middle Atlantic Bight (MAB) includes the continental shelf and slope region off the coast of Massachusetts (~42°N) to Virginia (~34°N) in the northwest Atlantic Ocean (Fig. 1B). At intermediate water depths, an oxygen minimum is located at ~1000 m with an oxygen content of ~140 μM (GEOSECS station 121, 35.59°N, 67.59°W; Fig. 2C). The BWO concentrations bathing the sediment cores used in this study range from ~190 μM to ~270 μM. The OCF in the region studied reaches a maximum of 2.4 g/cm^2 kyr at a water depth of ~1000 m (Anderson et al., 1994; Biscaye and Anderson, 1994). Most

of the organic carbon (C$_{org}$) deposited on the upper slope of the MAB sediments is supplied by lateral transport, mostly from the adjacent shelf (Anderson et al., 1994). Sediment accumulation rates in the region of the MAB studied range from 20 to 40 g/cm^2 kyr (Anderson et al., 1994).

3. SAMPLING AND EXPERIMENTAL METHODS

At each location (Table 1 and Fig. 1), either box coring or multicoring was used to collect sediment cores for pore-water and sediment analyses.

3.1. Sediment and Pore-Water Sampling

Most of the pore-water samples used here (SBB, SCB, California Margin) were extracted by sectioning sediment cores immediately upon retrieval in a nitrogen-filled glove bag in a refrigerated van kept at bottom-water temperature. Sectioned sediment from these cores was transferred to centrifuge tubes and capped before being removed from the glove bag for centrifugation. Centrifuged pore water was filtered through a 0.45-μm membrane filter in a separate nitrogen-filled glove bag. Pore waters from the MAB were obtained by the whole-core squeezing method of Jahnke (1988). Filtered pore-water samples were acidified to pH ~2 with Seastar ultrapure concentrated HCl within a month of the sampling after the samples were returned to shore-based laboratory.

3.2. Chemical Analyses of Dissolved Constituents

Analyses for metals (U and Fe) were performed on acidified and filtered water samples. The concentration of dissolved U in pore water (SBB) was measured by isotope dilution inductively coupled plasma-mass spectrometry (ICP-MS) by a method similar to that described by Toole et al. (1991) and by Colodner (1991). One hundred microliters of

A) Oxygen (μmole/kg)

B) Oxygen (μmole/kg)

C) Oxygen (μmole/kg)

SBB (34.25 °N, 120.03 °W)

California Margin GEOSEC sta 201
(34.10 °N, 127.53 °W)

SCB CalCOFI sta 9340 (32.52 °N, 118.22 °W)

Middle Atlantic Bight
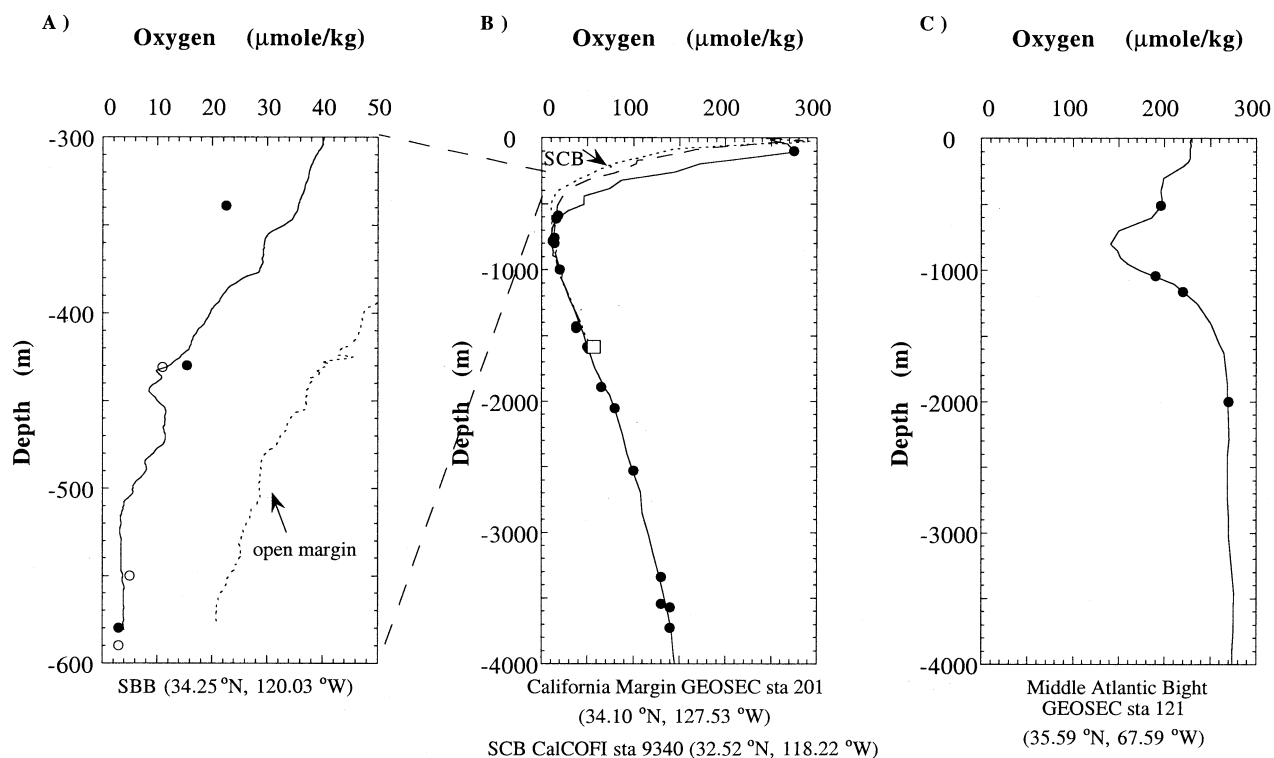GEOSEC sta 121
(35.59 °N, 67.59 °W)

Fig. 2. (A) Dissolved oxygen concentrations inside the SBB (thin solid line) below a depth of 300 m. The SBB data is measured by an oxygen sensor attached to the rosette conductivity-temperature-depth (CTD) on board the R/V *Pt Sur* during cruises in 1995 and 1997. The solid circles representing SBB data are means of triplicate micro-Winkler titrations by Dr. J. Bernhard on Niskin bottles triggered by the multicorer at depths of 340, 430, and 590 m during the November–December 1995 cruise, and the open circles are for the multicores at water depths of 430, 560, and 590 m during the April 1997 cruise. The thin dotted line is the dissolved oxygen profile obtained outside of the basin during the 1995 cruise (Kuwabara et al., 1999). The dashed lines show the region of the oxygen minimum zone from which the SBB profile is taken. (B) Dissolved oxygen depth profiles at 34°N, off the California Margin (GEOSECS station 201) and within the SCB (dotted line, August 1989; dashed line, August 1994). The SCB data are from CalCOFI station 9340. The oxygen concentration and depth of BC-20 from SCB is plotted as an open square. The depth of the cores from the California Margin are plotted as solid circles. (C) Dissolved oxygen depth profile at 35°N in the MAB (GEOSECS station 121). The depth of the cores from the MAB are plotted as solid circles.

water and an appropriate amount of isotope spike (^{236}U) were diluted to 10 mL in a matrix of 0.1% HNO$_3$ (Seastar) and equilibrated for over 24 h before measurement. The reproducibility is ~2% for U. The concentration of dissolved U in pore waters from the MAB, California Margin, and SCB was measured by isotope dilution thermal ionization mass spectrometry as described by Anderson et al. (1989b). Dissolved Fe concentrations in pore waters from SBB and the MAB were measured by graphite-furnace atomic absorption spectrometry.

3.3. Analyses of Solid-Phase Samples for U, Th, and ^{210}Pb

Isotope dilution ICP-MS methods for U and Th (with ^{236}U used as spikes for both U and Th) in SBB sediment are described by Zheng (1999). The long-term (over 1 yr) precision is ~3% for U and 4% for Th, which is based on 15 repeated analyses of a SBB sediment sample. Sediment samples from SCB and from certain California Margin cores at 35°N (BC151, BC150, BC106, and BC116; see Table 2), and from the MAB were analyzed for U and Th by alpha spectrometry. The precision of U and Th analyses by alpha spectrometry is ~5%. Sediment^{210}Pb was analyzed following the method of Anderson et al. (1988).

4. RESULTS: PORE-WATER U AND SEDIMENT U

4.1. SBB

We distinguish the SBB "slope" (<475 m) and "basin" (>475 m) sediments on the basis of several characteristic

differences. For example, basin sediments have higher porosity (>95%), lower in situ density, higher percentage of CaCO$_3$, and higher percentage of C$_{org}$ (Zheng, 1999). Basin sediments are laminated, whereas slope sediments are bioturbed (Hulsemann and Emery, 1963; Kuwabara et al., 1999). Sediment mass accumulation rates (MARs) for six SBB cores, obtained by means of ^{210}Pb, range from 65 to 240 g/cm^2 kyr (Table 1). Unsupported ^{210}Pb, as well as ^{234}Th results, indicate that the top ~12 cm of sediment from the site of core M590-3 had been removed some weeks before coring (Zheng et al., 2000).

Deep basin sediments are characterized by an intense redox gradient within a few centimeters of the sediment–water interface, resulting in overlapping of oxic, suboxic, and anoxic diagenetic reactions (Reimers et al., 1996). The deep basin site M580-2 displays the shallowest pore-water Fe maximum, at 1.7 cm, among all the sites studied here (Fig. 3). Near-zero pore-water Fe concentrations throughout core M590-3 (Fig. 3) are a relict feature of more reducing conditions normally found at greater sediment depth, consistent with loss of the top 12 cm of sediment (Zheng et al., 2000). Within the basin sites, one finds depth-related changes in redox intensity reflected best by the dissolved sulfide concentrations in pore waters. At the deep site

Table 1. Locations of sediment cores.

Site and date	Core	Latitude	Longitude	Depth (m)	Operation	MAR (g/cm² kyr)	Chronology	Reference for MAR
Santa Barbara Basin								
12/2/95	M340-2	34.3343	−119.8708	340	Multicoring-E	242	Pb-210	Zheng et al. (2000)
11/30/95	M430-2	34.3095	−119.9030	430	Multicoring-A	77	Pb-210	Zheng et al. (2000)
4/26/97	M430-3	34.3107	−119.9037	440	Multicoring-H	100	Pb-210	Zheng et al. (2000)
4/27/97	M550-3	34.2678	−119.9673	550	Multicoring-I	72	Pb-210	Zheng et al. (2000)
12/1/95	M580-2	34.2308	−120.0482	580	Multicoring-C	93	Pb-210	Zheng et al. (2000)
4/25/97	M590-3	34.2303	−120.0490	590	Multicoring-G	65	Pb-210	Zheng et al. (2000)
San Clemente Basin								
1/26/86	BC-20	32.5877	−118.2562	1585	Box coring			This study
1/7/85	QP-2	32.9067	−118.1650	NA	URI Quadropod	5.5	C-14	This study
California Margin								
7/16/88	BC208	35.6348	−121.6068	781	Box coring	6	C-14[a]	Gardner et al. (1997)
11/8/87	BC151	35.6333	−121.6167	786	Box coring	6	C-14[a]	Gardner et al. (1997)
11/8/87	BC150	36.1797	−122.3613	1566	Box coring	4	C-14[a]	Gardner et al. (1997)
10/28/87	BC106	36.1392	−122.4320	2033	Box coring	4	C-14[a]	Gardner et al. (1997)
10/31/87	BC116	36.1005	−122.5998	3319	Box coring	6	C-14[a]	Gardner et al. (1997)
7/23/88	BC231	35.5990	−122.3550	3728	Box coring	6	C-14[a]	Gardner et al. (1997)
Middle Atlantic Bight								
10/27/88	EN187-BC4	37.6222	−74.2217	512	Box coring	26	C-14[b]	Anderson et al. (1994)
10/27/88	EN187-BC5	37.6175	−74.1672	1045	Box coring	26	C-14[b]	Anderson et al. (1994)
10/29/88	EN187-BC9	36.8700	−74.5640	1165	Box coring	41	C-14[b]	Anderson et al. (1994)
10/28/88	EN187-BC6	37.4002	−73.8282	2000	Box coring	26	C-14[b]	Anderson et al. (1994)

[a] Adopt regional average values of sediment MAR (Gardner et al., 1997) for depth range of ~1000 m, 1500 to 2000 m, and >3000 m.
[b] C-14 dating was based on a nearby gravity core.

(580 m), sulfide concentrations exceed 0.1 μM right below the sediment–water interface and can be as high as 100 μM less than 10 cm depth downcore, increasing further to concentrations > 1000 μM at depths below 25 cm (Kuwabara et al., 1999). Yet at the shallow basin site (550 m), the sulfide concentration is only 0.05 μM at 10 cm (Kuwabara et al., 1999). The sediment redox gradient is much weaker on the slope, as evidenced by deeper Fe maxima (Fig. 3) and even lower sulfide concentrations (Kuwabara et al., 1999). The sulfide concentration is 0.02 to 0.04 μM at 10 cm downcore for the 430 m site and is <0.005 μM at 10 cm downcore for the 340 m site.

Despite the difference in redox gradients between basin and slope sites in the SBB, the extent of pore-water U depletion is similar at all sites, with U concentration decreasing from 12.5 nM to ~4 nM (Fig. 3). The prominent curvature in the pore-water U profiles coincides with the depth of the dissolved Fe peaks. The pore-water U gradient is smaller at the basin sites despite the more-reducing conditions that occur there. At present, we do not understand why the minimum pore-water U concentration is higher at the 580 m site than at the slope sites (Fig. 3), but a similar feature has been observed in some organic rich, sulfide-containing sediments in the Black Sea (Anderson and Fleisher, 1991; Barnes and Cochran, 1991).

The concentration of excess U over detrital background levels is greater in the basin cores (3 to 4 μg/g) than the slope cores (~2 μg/g). All profiles of uranium show at least 1 μg/g excess over the detrital background value right from surface-most sample of the sediment (Fig. 3).

4.2. SCB

The extent of pore-water U depletion (to ~4 nM) and enrichment of authigenic U (3.6 μg/g) in SCB sediment is similar to that of the SBB slope sites, even though the SCB site has a less intense redox gradient as indicated by a deeper pore-water Fe concentration maximum lying between 5 and 10 cm (Fig. 4). The low resolution of the pore-water U profile precludes detailed interpretation, but the curvature is consistent with U precipitation within the zone of Fe reduction, as was observed in SBB. The pore-water U profile suggests that precipitation of authigenic U may occur at depths as shallow as ~2.5 cm; however, the principal increase in authigenic U concentration does not occur until a depth of ~5 cm (Fig. 4).

4.3. California Margin

The extent of pore-water U depletion is also to ~4 nM in our profiles from two California Margin box cores collected at 35°N (profiles with open symbols in Fig. 5). Similar pore-water results have been reported before for this region (Klinkhammer and Palmer, 1991), and those data (profiles with solid symbols in Fig. 5) are replotted together with our new results. The pore-water U gradient change occurs at ~5 cm and clearly coincides with the maximum pore-water Fe concentration in the profiles from 781 m (solid symbols, Fig. 5). The pore-water U gradient change occurs at ~5 cm as well at 1585 m, but there are no pore-water Fe data for comparison. At 3728 m, the depth of the pore-water U gradient change is difficult to determine because the pore-water U profile is less smooth, but it seems that the lowest pore-water U concentration is found to coincide with the broad pore-water Fe maximum.

Concentrations of authigenic U increase with depth in the sediments, reaching levels of 2 to 4 μg/g (Fig. 5). Results from selected depths (11 cm and 19 cm) of a larger number of cores from the California Margin, also at ~35°N (Zheng, 1999), are generally consistent with the more detailed profiles shown here.

Table 2. U mass budget in the SBB, SCB, California Margin, and MAB sediments.

| Site and core | Water depth (m) | [O₂]ᵃ (μM) | [H₂S]ᵇ (μM) | Supply (μg/cm² kyr) | | | Focusing factorf (ψ) | U MAR (μg/cm² kyr) | | |
				Diffusive fluxᶜ (F_{diffU})	Estimated fluxᵈ (F_{PNU})	Corrected fluxᵃ (F*_{PNU})		Totalᵍ (MAR_{Uauth})	Precipitation in situʰ (MAR^{insitu})	Remobilized fluxⁱ (F_{remobU} μg/cm² kyr)
Santa Babara Basin										
M340-2	340	23	0.005	264	91	315	2.9	443	128	135
M430-2	430	15	0.040	319	91	100	0.8	147	46	273
M430-3	440	11	0.025	362	91	130	1.1	227	97	265
M550-3	550	5	0.050	*186*	91	94	1.6	302	209	
M580-2	580	3	100	*37*	91	121	1.9	251	130	
M590-3	590	3	500	*89*	91	85	1.3	181	97	
San Clemente Basin										
BC20		57		37	3			20		20
California Margin										
BC208	781	12		86	16			12		90
BC151	787	12			16			18		
BC150	1585	50		33	10			11		32
BC106	2055	80			10			14		
BC116	3340	130			4			18		
BC231	3728	140		20	4			20		4
Middle Atlantic Bight										
EN187-BC4	512	200		54	0			16		38
EN187-BC5	1045	190		20	0			24		−4
EN187-BC9	1165	220		18	0			64		−45
EN187-BC6	2000	270		28	0			19		10

ᵃ Dissolved oxygen in bottom water at core site (Zheng et al., 2000, CALCOFI; Reimers et al, 1992, GEOSECS).
ᵇ Sulfide concentration in pore waters at 10-cm depth (Kuwabara et al., 1999).
ᶜ Diffusive flux estimated based on U concentration gradient in pore waters; fluxes at basin sites (italic) are underestimated.
ᵈ Particulate nonlithogenic U flux estimated based on sediment trap U flux (Zheng et al., 2002).
ᵉ Particulate nonlithogenic U flux corrected for sediment focusing (see text).
ᶠ Sediment focusing factor (Zheng et al., 2000).
ᵍ Burial rate of authigenic U estimated from average authigenic U concentrations and bulk sediment MAR (Table 1).
ʰ Burial rate of authigenic U that is precipitated in situ, equals to total MAR_{Uauth} minus F_{PNU}, or, where available, F*_{PNU}.
ⁱ Flux of U remobilized estimated using Eqn. 4; large negative value for EN187-BC9 may result from underestimate of F_{PNU} at this site.

4.4. MAB

Pore-water U concentration profiles display a drop from the seawater value to a minimum value of ~2 nM at ~5 cm depth down core in all MAB cores (Fig. 6). In comparison, in SBB, SCB and California Margin cores, pore-water U concentration drops to ~4 nM at depths. We do not know whether this difference between west coast (4 nM) and east coast (2 nM) is because the MAB pore waters were sampled by whole core squeezing, whereas the others were by centrifugation. However, the U concentration gradients in the MAB profiles (Fig. 6) are similar to those observed at California Margin sites (Fig. 5) but are less than those observed at SBB slope sites (Fig. 3). The sediment redox gradients are less intense at the MAB sites compared with SBB, exhibiting a more expanded region of the suboxic zone as indicated by deeper Fe pore-water maxima at depths ranging from 5 to 10 cm (Fig. 6). The maximum curvature in pore-water U profiles, indicating the depth of authigenic U precipitation, occurs at the depth of the pore-water Fe maxima, or at a slightly shallower depth.

All sites show solid phase authigenic U enrichment of 0.5 to 2 μg/g above detrital background values, although the extent of the enrichment differs from site to site, as does the shape of the sedimentary authigenic U profile (Fig. 6). The "fluff" layer from the 1045 m site contains 1.8 μg/g of PNU (Zheng et al.,

2002), but this U is oxidized rapidly and is lost to the water column because the core-top sediment shows no enrichment of U (Fig. 6).

4.5. Maximum Downward Diffusive Fluxes of U at All Sites

Diffusive fluxes of U into the sediments were calculated by the following equation:

$$\text{Flux} = D_{UO_2^{2+}} (T°C) \times \phi^n \times \frac{\Delta U}{\Delta z} \qquad (1)$$

where ϕ represents porosity and $\Delta U/\Delta z$ is the pore-water U gradient over the interval where the maximum gradient is observed. We adopt value of 2 for n to account for the tortuosity of the sediment. When pore-water U concentration profiles decreases continuously with depth, the pore-water gradient for U is calculated by taking the difference between the U concentration at the depth of the first sampling point in the sediment and that of the overlying water, divided by the first sampling depth. In the case when there is a subsurface peak of pore-water U, the pore-water gradient for U is calculated by taking the difference between the peak U concentration and that of a sample below the subsurface U peak. This procedure
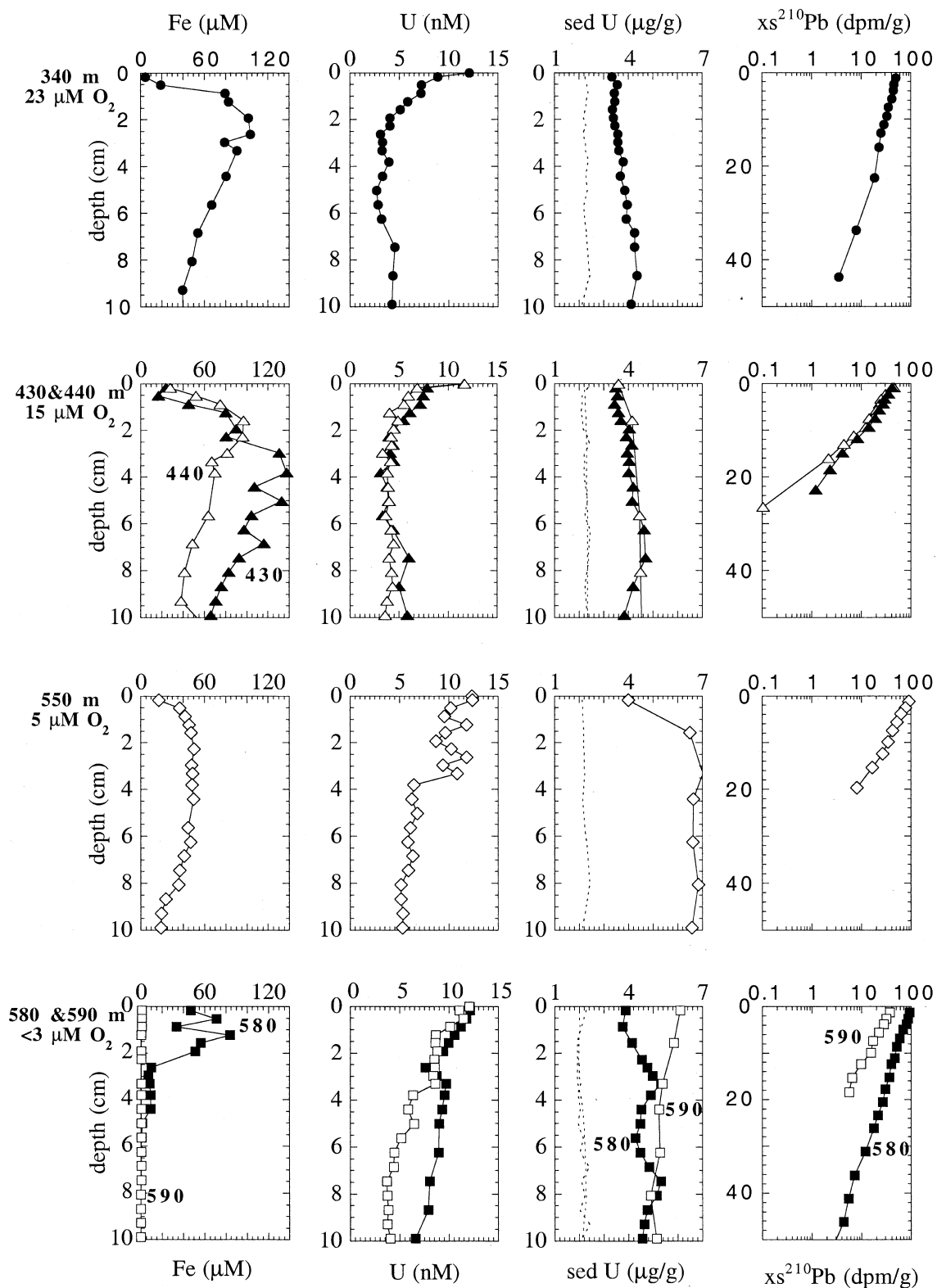
Fig. 3. Depth profiles of Fe and U in pore waters, and solid phase U in the upper 10 cm at four sites at nominal depths of 340 m, 430 and 440 m, 550 m, and 580 and 590 m along the northeast flank of the SBB. Profiles of unsupported [210]Pb (xs[210]Pb) are shown to a depth of 50 cm. The values for overlying water drawn at ~10 cm above the sediment–water interface are plotted at 0 cm in all pore-water profiles. Data from cruises in November–December 1995 and in April 1997 are shown by solid and open symbols, respectively. In panels showing the sediment U profiles, the dotted lines indicate the calculated detrital background values of U on the basis of the [232]Th concentration of the sediment assuming that the detritus has a U/Th ratio of 0.2123 (g/g).
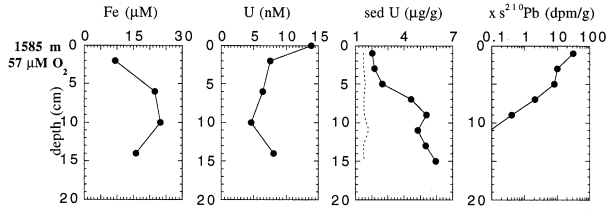
Fig. 4. Depth profiles of pore water dissolved Fe, U, sediment U, and unsupported ^{210}Pb in the upper 20 cm of SCB core BC-20. Plotted at 0 cm in the pore-water U profile is the bottom-water U concentration. In the sediment U profile, the dotted line indicates the calculated detrital background values of U on the basis of the ^{232}Th concentration of the sediment, assuming that the detritus has a U/Th ratio of 0.2123 (g/g) (Taylor and McLennan, 1985).

allows us to obtain the maximum downward diffusive U flux at all sites, which is the parameter required to evaluate U remobilization by means of a mass budget approach (see below). The molecular diffusivity $D_{UO_2^{2+}}$ at bottom-water temperature (T°C) is calculated by the Stokes-Einstein diffusion coefficient temperature dependence described by Li and Gregory (1974) and the estimated UO_2^{2+} diffusion coefficient at 25°C of 4.26×10^{-6} cm^2/s (Li and Gregory, 1974):

$$D_{UO_2^{2+}}(T°C) = \frac{D_{UO_2^{2+}}(25°C)}{2.19}$$
$$+ \frac{T}{25} \times \left(D_{UO_2^{2+}}(25°C) - \frac{D_{UO_2^{2+}}(25°C)}{2.19} \right) \quad (2)$$

In the SBB, the U diffusive flux at the slope sites ranges from 260 to 360 μg/cm^2 kyr (Table 2), but is much lower at the basin sites with a range of 40 to 190 μg/cm^2 kyr (Table 2). A diffusion coefficient corresponding to the bottom-water temperature of 6°C (2.5×10^{-6} cm^2/s) is used for the diffusive flux calculation.

In the SCB, the diffusive flux of U is ~40 μg/cm^2 kyr for BC-20 (Table 2). This estimate is not too different from published estimates of the diffusive U flux (24 to 32 μg/cm^2 kyr) to SCB sediments on the basis of in situ harpoon pore-water U profiles (Barnes and Cochran, 1988, 1990). However, these diffusive fluxes represent minimum estimates due to the low-resolution sampling of BC-20 (Fig. 4) and by the harpoon, which has the first pore-water sample taken at a 2.5 cm depth (Barnes and Cochran, 1990).

In California Margin sediments, the U diffusive flux for BC-208, located in the oxygen minimum zone, amounts to 90 μg/cm^2 kyr on the basis of our calculation, and is estimated to be 100 μg/cm^2 kyr by Klinkhammer and Palmer (1991), who used a slightly different diffusion coefficient of U (Table 2). The U diffusive flux for BC-150, from a site exposed to 50 μM bottom-water oxygen, is ~30 μg/cm^2 kyr, reflecting a less intense redox gradient at this site (Reimers et al., 1992). The U diffusive flux for BC-231, exposed to 140 μM BWO is ~20 μg/cm^2 kyr, reflecting the least intense redox gradient at this site (Reimers et al., 1992). In the MAB, the diffusive fluxes of U range from 20 to 50 μg/cm^2 kyr (Table 2). As for the SCB, these fluxes represent lower limits due to the low sampling resolution of the pore-water U profiles (Fig. 6).

4.6. Accumulation (Burial) Rates of Authigenic U

Accumulation rates of authigenic U were calculated by the following equation:

$$MAR_{U_{auth}} = [U_{auth}] \times MAR_{sed} \quad (3)$$

where $[U_{auth}]$ is the average authigenic U concentration from the depth where pore-water Fe reaches its maximum concentration to ~30 cm downcore (or to the maximum depth of core if its length is shorter than 30 cm) and MAR_{sed} is the bulk sediment MAR (Table 1).

In the SBB, the accumulation rate of authigenic U ranges from 147 to 443 μg/cm^2 kyr (Table 2). In the SCB, the accumulation rate of authigenic U in BC-20 is 20 μg/cm^2 kyr (Table 2). On the California Margin, the sediment authigenic U MAR ranges from 10 to 20 μg/cm^2 kyr (Table 2). Sediment MAR values for California Margin cores are mostly based on radiocarbon chronology (Reimers et al., 1992; Gardner et al., 1997), and we use the average values of 6, 4, and 6 g/cm^2 kyr (Table 1) for three depth intervals: oxygen-minimum zone (600 m to 1000 m), 1400 m to 2000 m, and 3300 m to 4000 m, to reflect the general sedimentation patterns obtained on many cores from that region (Gardner et al., 1997). In the MAB, authigenic U accumulation rates range from ~20 to ~70 μg/cm^2 kyr (Table 2).

5. DISCUSSION

In each of the regions studied, pore-water U profiles show evidence for authigneic U precipitation within the zone of bioturbation, as inferred from the unsupported ^{210}Pb profiles. Subsequent mixing of authigenic U-containing sediments upward into more oxidizing conditions, as a result of bioturbation, is expected to cause oxidative remobilization of some portion of the authigenic U. A mass balance approach is used here to estimate the amount of U remobilized and lost from the sediments at each site.

5.1. Mass Budget Constraints

To estimate the fraction of authigenic U that is eventually preserved and buried, a mass budget for U was constructed at each site as follows:

$$MAR_{U_{auth}} = F_{PNU} + F_{diffU} - F_{remobU} \quad (4)$$

where $MAR_{U_{auth}}$ is the accumulation rate of total nonlithogenic U (this includes PNU formed in surface waters together with authigenic U precipitated in situ under reducing conditions; section 4.6); F_{PNU} is the flux of PNU that is preserved and buried (Zheng et al., 2002); F_{diffU} is the diffusive flux of U into sediments calculated from pore-water concentration profiles (section 4.5); and F_{remobU} is the flux of authigenic U back to the water column after oxidative remobilization. Implicit in our mass budget approach is the assumption that the system is at steady state over timescales for which sediment burial is evaluated—that is, 100 to 1000 yr. Remobilization is likely to be an intermittent process because of the stochastic nature of bioturbation (Wheatcroft et al., 1990). Therefore, the probability of observing an efflux from the sediments of remobilized U in any one core is quite low, and the average flux of remobilized U is
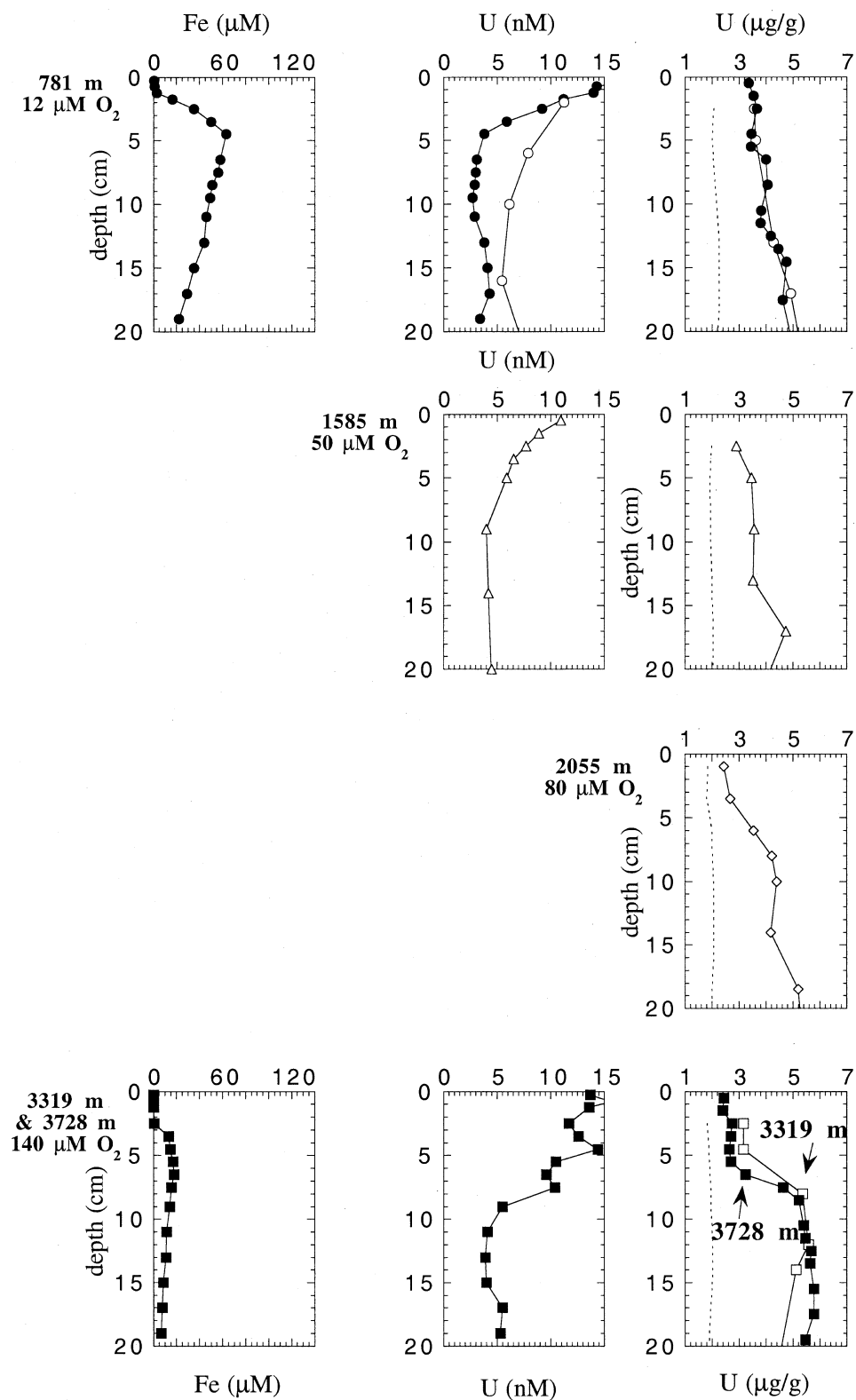
Fig. 5. Depth profiles of dissolved Fe and U in pore water, together with solid-phase U in the upper 20 cm of sediments at sites near 35°N along the California Margin. Solid symbols in pore-water Fe, U, and sediment U concentrations plots represent the data of Klinkhammer and Palmer (1991). The open symbols in pore-water U and sediment U concentrations plots are from this study (see Table 1 for locations). A solid-phase U profile at 3319 m from this study has been plotted together with the profile from Kinkhammer and Palmer (1991) at 3728 m. The dotted lines in the sediment U concentration plots indicate the calculated detrital background values of U on the basis of the [232]Th concentrations, assuming that the detritus has a U/Th ratio of 0.2123 (g/g).
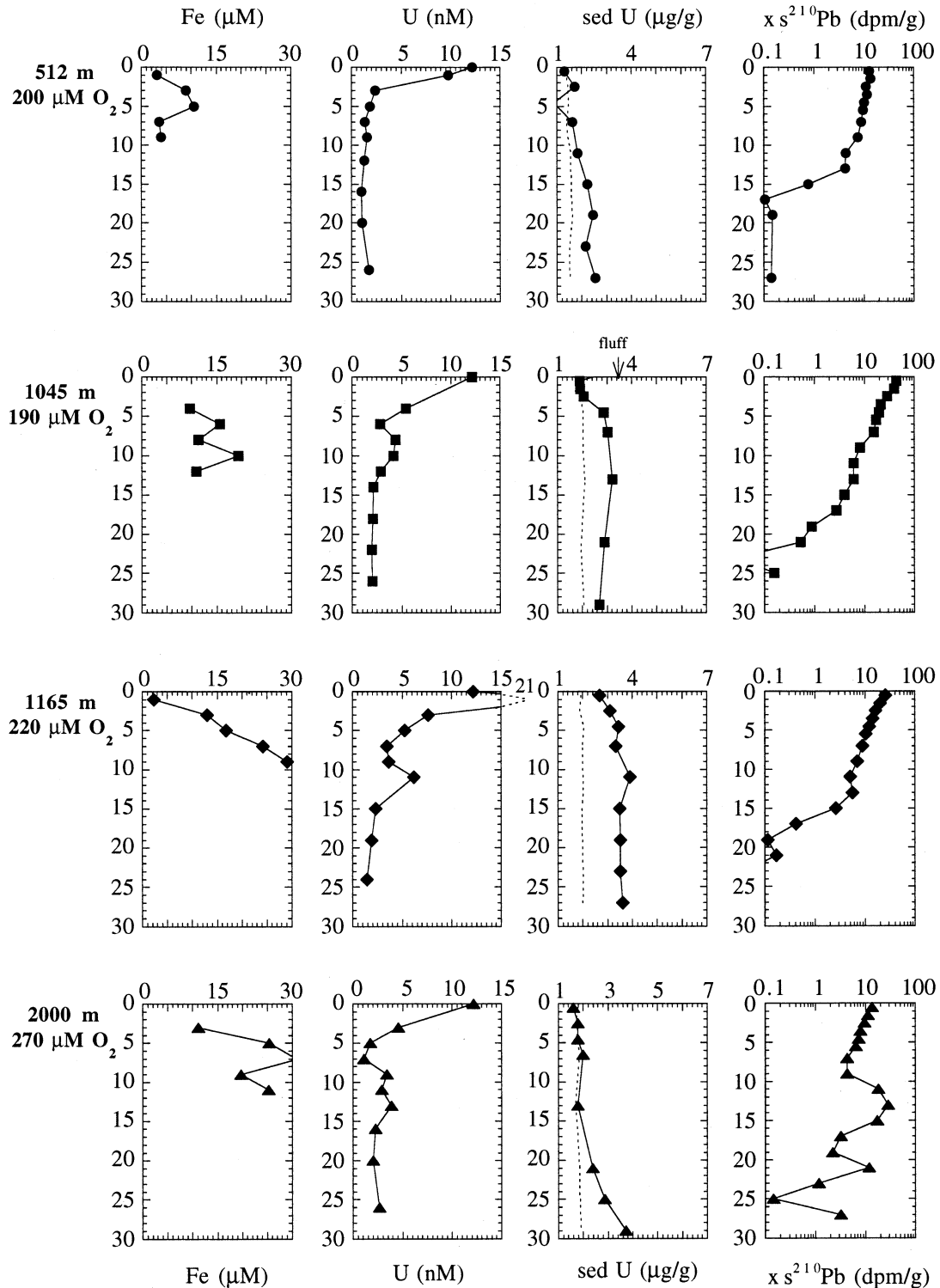
Fig. 6. Depth profiles of pore-water Fe and U concentrations, sediment U concentration, and unsupported ^{210}Pb in the upper 30 cm of MAB box cores recovered during cruise EN 187 (Table 1). The thin dotted lines in the panel showing sediment U profiles indicate calculated detrital background values of U on the basis of the ^{232}Th concentration of the sediment assuming an end member ratio of U/Th of 0.2123 (g/g).

calculated by difference after evaluating each of the other parameters, for which values are presented in Table 2.

The diffusion flux and burial rate of authigenic U are com-

bined with particulate U fluxes obtained at different sites that bear first-order similarities but that are sometimes as much as several hundred kilometers from the sites at which diffusive

flux and burial rate are evaluated. For example, in the SBB, a sediment trap located right above the 590-m basin site in the center of the basin was used to represent PNU input to both basin and slope sites. In the MAB, sediment trap data from ~39.5°N and ~35.5°N are used to constrain the particulate U input flux for core sites at ~37°N. In the northeast Pacific, off of northern California, sediment trap data from 42°N are used with results from cores taken along a transect down the continental slope at ~35°N. Although combining results from geochemically similar but geographically separated sites is less than ideal, this is the best that can be done in most cases with existing data.

The flux of PNU (F_{PNU}) preserved and buried at each site was evaluated by Zheng et al. (2002) and is reproduced in Table 2. Within the SBB, F_{PNU} must be adjusted for sediment focusing, which is pronounced at the sites studied (Zheng et al., 2000). We assume that particles redistributed laterally by sediment focusing have a PNU content equal to that of annual-average sediment trap samples. This assumption is supported by the fact that the concentration of authigenic U in surface-most sediments at each of the SBB slope sites (Fig. 3) is equal to the annual average concentration of PNU in sediment trap samples (1.3 $\mu g/g$), despite nearly a fourfold range of sediment focusing factors among these sites (Table 2). The focusing-corrected F_{PNU} (F^*_{PNU}) is then

$$F^*_{PNU} = MAR_{sed} \cdot U^{trap}_{PNU} \qquad (5)$$

where MAR_{sed} is the sediment accumulation rate at each site (Table 1) and U^{trap}_{PNU} is the annual average PNU concentration of the sediment trap samples. The focusing-corrected F_{PNU}, F^*_{PNU}, is used in Eqn. 4 to estimate F_{remobU} in the SBB (Table 2).

No correction is made for sediment focusing at the other sites. Although extensive sediment focusing occurs in the MAB (Anderson et al., 1994), preservation of PNU is negligible, so no correction is needed, except perhaps for the 1165-m site, where the sediment U profile suggests that PNU could account for a large fraction of U buried (Fig. 6). At the other sites studied, we have no information with which to evaluate sediment focusing factors, so corrections for focusing are not made. However, because fluxes of PNU are generally much less than the diffusive flux of U into the sediments at these sites (Table 2), neglecting the effects of sediment focusing is unlikely to introduce errors that significantly alter our conclusions.

A consistent feature emerges from the U mass budgets. Authigenic U preservation is fairly poor even under bottom-water oxygen concentrations as low as 15 μM, as indicated by the imbalance of the U budget (i.e., expressed as F_{remobU} in Table 2). The magnitude of this sedimentary authigenic U imbalance ranges from one-third to two-thirds of the total input.

Large uncertainties are inherent in our evaluation of authigenic U preservation, in part because it was necessary to evaluate PNU fluxes at sites somewhat distant from the locations of cores used to determine diffusive fluxes and burial rates of authigenic U. Nevertheless, our estimated fluxes of U to the sediments are generally conservative (i.e., lower limits), so our computed values represent lower limits for F_{remobU}. For example, the diffusive flux of U into sediments at sites in the MAB and in SCB are underestimated substantially because the sam-

pling resolution of the pore-water U profiles at these sites is low. To illustrate the potential magnitude of the error introduced by the low sampling resolution at these sites, we recalculated the diffusive fluxes at the SBB sites by using selected pore-water data at a resolution equivalent to that available for SCB and MAB profiles. Recalculated U fluxes for the SBB sites are less than one-fifth of the values reported in Table 2. Consequently, the flux of U remobilized from SCB and MAB sediments is likely to be much greater than reported in Table 2; that is, the preservation efficiency of authigenic U at these sites may be substantially less than our conservative estimates. Despite the unquantifiable uncertainties associated with evaluating long-term average diffusive fluxes and burial rates at any single site, the fact that imbalances in the U budget are consistently found in many and diverse environments indicates that periodic remobilization of authigenic U is a common occurrence and a robust result.

5.2. Role of Bioturbation

Two possible explanations exist for the large imbalances in the U budgets at the sites studied. The first is that diffusive fluxes of U into the sediments have been enhanced in recent years, perhaps because of climate variability or human impact (eutrophication). The second is that diffusive fluxes do not represent steady-state conditions over the timescale of 100 to 1000 yr (i.e., the timescale over which burial is evaluated) because a large fraction of authigenic U precipitated within the sediment is periodically remobilized by the actions of bioturbating organisms.

Several lines of evidence favor the second explanation. First, it would be unlikely that decadal climate variability or human impacts caused OCFs to be higher than average at all of the sites studied at exactly the times when our samples were collected. Second, sites at which regeneration of authigenic U occurs (Table 2) all show evidence of bioturbation. Unlike the deep basin sediments of SBB, slope sediments are unlaminated, indicating mixing by bioturbation. Unsupported ^{210}Pb profiles (Fig. 3) indicate bioturbation to depths >2 cm at SBB slope sites. In SCB, the pore-water U profile (Fig. 4) indicates that authigenic U should precipitate at a depth of ~2.5 cm, yet the sediment profile shows that the most prominent increase of authigenic U concentration starts at a depth >5 cm. The unsupported ^{210}Pb profile also displays a change of gradient at 5 cm (Fig. 4), indicating that the principal accumulation of authigenic U occurs below the zone of rapid bioturbation. Along the California Margin, bioturbation depth is probably ~5 cm as well. The prominent increase of sediment U concentration at ~7 cm for the core at 3728 m, together with the erratic pore-water U profile at this site (Fig. 5), suggests periodic and, perhaps, recent remobilization of U. In the MAB, bioturbation to >15 cm depth also leads to remobilization of authigenic U, as best illustrated at 2000 m, where the concentration of authigenic U only begins to increase at a depth ≥10 cm below the zone of most active U precipitation (5 to 7 cm), as indicated by the pore-water U profile (Fig. 6). These results all indicate that bioturbation inhibits the preservation of authigenic U.

Our proposed mechanisms for remobilization of authigenic U by bioturbation is similar to that proposed for remobilization and oxidation of solid sulfide to dissolved sulfate (Aller, 1980).

Bioturbation transports upward authigenic U-containing sediment from a level where authigenic U is thermodynamically stable to a shallower level (sediment–water interface, or oxygenated sediment interval) where it is not. Oxidation of thermodynamically unstable authigenic U generates a "reversed" pore-water U concentration gradient, leading to an efflux of dissolved U from sediments into the overlying bottom water. Such "reversed" pore-water U profiles are observed occasionally (Barnes and Cochran, 1990) and are consistent with our proposed mechanism, even though there are insufficient data to present a statistical analysis of the episodic bioturbation effect.

Numerous experimental studies have shown that authigenic U in marine sediments is labile toward remobilization when exposed to oxygen (Toole et al., 1984; Cochran et al., 1986; Anderson et al., 1989b). Authigenic U is also mobilized during the "burn-down" (oxygen penetration) of turbidites (Colley et al., 1989) and sapropels (Thomson et al., 1995). Our results are consistent with these studies in that as bioturbation raises upward deep, reducing, U-rich sediments, exposure to more oxidizing conditions leads to remobilization of authigenic U. Consequently, geochemical models used to reconstruct sediment redox conditions cannot equate the burial rate of authigenic U with the rate of U diffusion into sediments, the latter term being regulated by the depth of the redox level at which U is precipitated. Accurate reconstruction of sedimentary redox conditions that is based on the burial rate of authigenic U will require some means of estimating bioturbation parameters (rate and depth) together with the corresponding flux of U remobilized and lost to overlying bottom water.

5.3. Threshold Oxygen Level for Authigenic U Remobilization

Exposure of U-rich sediments to conditions characteristic of the sediment–water interface at the deepest "basin" site in the SBB (<3 μM BWO; >0.1 μM sulfide in pore waters) does not lead to remobilization of sedimentary authigenic U. Core M590-3 provides a serendipitous opportunity to constrain the chemical conditions under which authigenic U is remobilized. Sediments at the site of core M590-3 suffered a loss of the top 12 cm some days to weeks before the collection of our core, as evidenced by the presence of a small but detectable ^{234}Th inventory (1.5 dpm/cm^2) and concentration ($\sim$10 dpm/g) at <1 cm depth in this core (Zheng et al., 2000). It is unclear whether this loss was due to a natural erosion event or dredging and sampling activities in this heavily sampled area (Zheng et al., 2000). The smooth unsupported ^{210}Pb profile suggests that disturbance of the sediment recovered in core M590-3 was minimal (Fig. 3). Despite the exposure of sediment rich in authigenic U at the sediment–water interface (Fig. 3) for a period of days, if not weeks, little U remobilization has occurred since the exposure. The solid-phase authigenic U concentration in perturbed core M590-3 is the same as in the unperturbed core M580-2 at an equivalent age on the basis of ^{210}Pb chronology (Zheng, 1999). In addition, the pore-water U profile from M590-3 is also similar to that from the undisturbed nearby core M580-2 (Fig. 3).

In contrast to the deep basin conditions, exposure of U-rich sediments to bottom waters at the "slope" sites of SBB (15 to 25 μM BWO) leads to remobilization of sedimentary authigenic U. The large imbalance in the U mass budget (F_{remobU} $\sim$200 μg/cm^2 kyr) at the "slope" sites indicates that U is regenerated at these sites (Table 2). Therefore, the threshold oxygen level for remobilization of authigenic U is <15 μM, the value at the 430-m site.

5.4. Authigenic U Formation Mechanism

5.4.1. Coupling of Fe and U Reduction

One remaining unknown factor concerning U geochemistry is the redox potential at which U is reduced and precipitated. Some investigators have proposed that it occurs together with Fe(III) reduction (Cochran et al., 1986); others have concluded that more reducing conditions are required, such as when sulfate reduction occurs (Klinkhammer and Palmer, 1991). We can address this question by using our pore-water data, which consistently show that the change of pore-water U gradient occurs at the depth of the pore-water Fe maximum (Figs. 3 to 6). The substantial decrease of pore-water U concentration from the bottom-water value ($\sim$13 nM) to a constant pore-water U concentration of 2 to 4 nM is accomplished above the depth where the pore-water Fe concentration maximum is reached, indicating that most of the U reduction occurs at the redox potential where reduction of Fe(III) to Fe(II) occurs. However, this does not imply that reduction of U cannot occur under more reducing conditions when sulfate is reduced.

The relative importance of the reactions that reduce U at the Fe-reduction redox potential, and the reactions that reduce U at the more reducing sulfate-reduction redox potential, can be assessed from a comparison of the accumulation rate of U precipitated in situ, $MAR_{U_{auth}}^{in\ situ}$ (the total authigenic U MAR, $MAR_{U_{auth}}$, minus the focusing-corrected particulate nonlithogenic fluxes, F_{PNU}^*), from SBB slope sites (340 and 430 m) and basin sites (550 and 580 m). The fundamental difference of redox states is that sulfate reduction is much more prominent at the 580-m basin site, as indicated by highly elevated sulfide concentrations ($\sim$100 μM at 10 cm) compared with <0.05 μM at a 10-cm depth at the slope sites (Table 2; Sholkovitz, 1973; Kuwabara et al., 1999).

Sulfate reduction plays a limited role in augmenting the $MAR_{U_{auth}}^{in\ situ}$ in the SBB. For example, despite much more sulfidic conditions, the $MAR_{U_{auth}}^{in\ situ}$ at the deep basin sites (580 and 590 m) is comparable to that of the slope sites (340 and 430 m; Table 2), where Fe-reducing conditions prevail. Lack of enhancement of $MAR_{U_{auth}}^{in\ situ}$ at the deep basin sites suggests that conditions dominated by sulfate reduction are no more effective than conditions dominated by Fe reduction at burying authigenic U. In addition, the overall rate of Fe reduction is probably inhibited at the deep basin sites, where reduced Fe is lost as Fe-sulfide near the sediment–water interface. In contrast, at the slope sites, Fe(II) produced by Fe-reducing bacteria diffuses upward, where it is reoxidized by oxygen, providing fresh Fe-oxyhydroxide to be used again and again. The abundant supply of fresh Fe-oxyhydroxide can catalyze U reduction either via enzymatic pathways (Lovley et al., 1991; Fredrickson et al., 2000) or via inorganic pathways (Liger et al., 1999).

5.4.2. Evidence for Microbially Mediated U Reduction

Reduction of U in marine sediments by inorganic reactions and by microbially mediated enzymatic reduction have both

Table 3. Fluxes of particulate carbon and uranium, bottom water composition,

Basin	C flux[a] (g/cm² kyr)	PNU[b] (μg/g)	PNU flux[b] (μg/cm² kyr)	Sulfide[c] (μM)	BW U[d] (nM)	Auth U[e] (μg/g)	U MAR (μg/cm² kyr) Total[f] (MAR$_{U_{auth}}$)	Precipitated in situ[g] (MAR^{insitu})
Framvaren Fjord	2			8000	6.0	14	126	
Black Sea	0.9	0.4–1.7	1.6–3.7	400	5.6	14	70	68
Cariaco Basin	0.7	0–0.3	NA	50	12.6	6	78	~80
Saanich Inlet	4.3	1.8–2.9	270–384	30	9.5	6	595	~300
Santa Barbara Basin	2.8	1–2.2	91	0	13	2.7	150–300	50–200

[a] Sediment trap flux at the deepest water depth; references for each basin in sequence are as follows: Næs et al. (1988), Muramoto et al. (1991), Thunell (unpublished data), Anderson et al. (1989b) and Thunell et al. (1995).

[b] Particulate nonlithogenic U (PNU) concentrations and fluxes; references for each basin in sequence are as follows: not available, Anderson et al. (1989a), Anderson (1987), Anderson et al. (1989b), and Zheng et al. (2002).

[c] Maximum concentration in bottom water; Saanich Inlet is seasonally anoxic. References are as follows: Skei et al. (1988), Murray et al. (1989), Scranton et al. (1987), Crusius et al. (1996), and Kuwabara et al. (1999).

[d] Bottom water U concentration; references in sequence are as follows: Todd et al. (1988), Anderson et al. (1989a), Anderson (1987), Todd et al. (1988), and this study.

[e] Sediment authigenic U concentration; references for each basin in sequence are as follows: McKee (unpublished data), Anderson and Fleisher (1991) and Barnes and Cochran (1991), Anderson (1987), Kolodny and Kaplan (1973), and this study.

[f] Accumulation rate of total nonlithogenic U, calculated using Eqn. 3. References for sediment MAR (data not shown) for each basin, in sequence, are as follows: Næs et al. (1988), Crusius and Anderson (1992), Anderson (unpublished data), Anderson et al. (1989b), and this study.

[g] Accumulation rate of authigenic U precipitated in situ.

been proposed. Reduction of U is probably not by simple inorganic reactions in solution, because reduction of soluble U(VI) to insoluble U(IV) is not observed to occur in the sulfide-containing water columns of anoxic marine basins (Anderson, 1987; Todd et al., 1988; Anderson et al., 1989a) despite thermodynamically favorable conditions (Langmuir, 1978). The limiting steps in the reduction of U(VI) to U(IV) could be the requirement of particle surfaces to catalyze the inorganic reaction (Kochenov et al., 1977; Liger et al., 1999) or the presence of enzymes associated with iron and sulfate reducing bacteria capable of reducing U. Dissimilatory sulfate and iron reducing bacteria have been shown to reduce U in laboratory culture experiments (Lovley et al., 1991, 1993; Lovley and Phillips, 1992; Fredrickson et al., 2000); however, the importance of microbially mediated U reduction mechanisms is difficult to demonstrate in nature.

Support for the importance of microbial U reduction in marine sediments can be found by comparing the authigenic U MAR in several anoxic basins, together with SBB. These basins exhibit a range of bottom-water sulfide concentrations and carbon flux to the sediment, as captured by the deepest sediment trap deployed in each basin (Table 3). Total sediment authigenic U MAR displays an increasing trend with increasing carbon flux (Fig. 7). More importantly, the MAR of authigenic U precipitated in situ, MAR$_{U_{auth}}^{in\ situ}$, estimated for each basin as described above, displays an increasing trend with increasing carbon flux as well (Fig. 7). The MAR$_{U_{auth}}^{in\ situ}$ is the highest (~300 μg/cm² kyr) in Saanich Inlet with a carbon flux of 4.3 g/cm² kyr (Anderson et al., 1989b), and is much lower (<80 μg/cm² kyr) in the Cariaco Basin (Anderson, 1987) with a carbon flux of 0.7 g/cm² kyr (R. Thunell, personal communication), despite the fact that both basins have similar bottom-water sulfide concentrations (Table 3), and that Saanich Inlet is only seasonally sulfidic (Crusius et al., 1996). The fact that the MAR of authigenic U precipitated in situ is positively correlated with the carbon flux to the sediment, but is not correlated with redox conditions in bottom waters, suggests that the rate of authigenic U formation is regulated by the rate of anaerobic bacterial metabolism; specifically, by the combined rates of iron reduction and sulfate reduction, rather than by inorganic reactions whose rates are regulated by the redox conditions of bottom waters.

6. CONCLUSIONS

Studies of pore-water and solid-phase U geochemistry in SBB, in SCB, along the California Margin, and in the MAB, in conjunction with the evaluation of particulate U fluxes at these locations by using sediment traps, allow us to make the following general conclusions regarding the processes regulating the formation, preservation, and burial of authigenic U:

(1) Bioturbation remobilizes authigenic U in marine sediments by raising U-containing reducing sediments up into a more oxidizing zone where oxidation of authigenic U leads to its remobilization. Mass budgets of authigenic U constructed for several sites reveal that a substantial amount (one-third to two-thirds) of the authigenic U formed in sediments is later remobilized and lost back to the water column. Remobilization occurs even when bottom-water oxygen concentrations are low (~15 μM) and OCFs are high, as in the case of the SBB slope sites.

(2) The redox cycling of U in marine sediments is closely coupled with the redox cycling of Fe. Reduction of U occurs at a redox potential similar to that of Fe reduction. Within the SBB, sites with pronounced sulfate reduction are no more effective at burying authigenic U than are sites where Fe reduction is the dominant anaerobic respiration process.

(3) Among a number of anoxic basins, the accumulation rates of authigenic U precipitated in situ show a clear positive correlation with OCF but do not show a correlation with bottom-water redox conditions, suggesting that microbially mediated U reduction is more important than inorganic chemical reactions as the mechanism responsible for precipitation and burial of authigenic U.
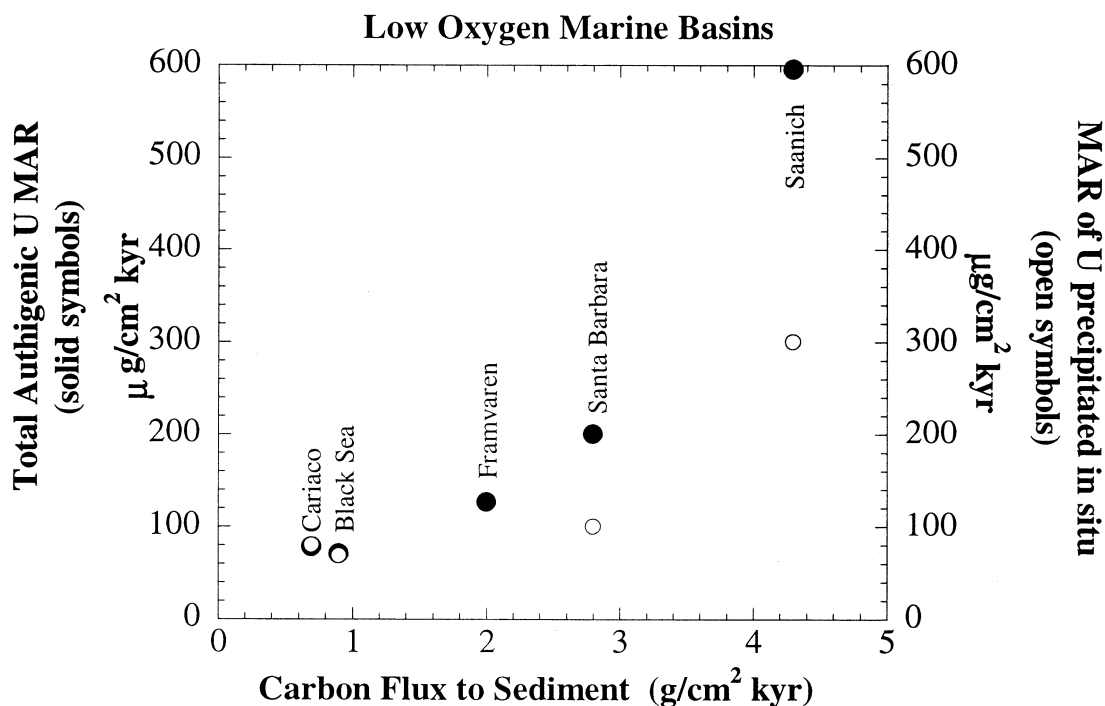
Fig. 7. Compiled data (Table 3) of total authigenic U MAR (solid symbols; includes PNU) in a series of anoxic basins plotted vs. the corresponding C_{org} flux to the sediment in each basin. Open symbols indicate the accumulation rate of U precipitated in situ, $MAR_{U_{auth}}^{in\ situ}$, estimated as total authigenic U MAR minus the flux of PNU preserved and buried at each site (Kolodny and Kaplan, 1973; Scranton et al., 1987; Næs et al., 1988; Skei et al., 1988; Murray et al., 1989; Muramoto et al., 1991; Crusius and Anderson, 1992; Zheng et al., 2002).

REFERENCES

Aller R. C. (1980) Diagenetic processes near the sediment–water interface of Long Island Sound: I. Decomposition and nutrient element geochemistry (S, N, P). In *Estuarine Physics and Chemistry: Studies in Long Island Sound, Advances in Geophysics,* Vol. 22 (ed. B. Saltzman), pp. 351–415. Academic Press, New York.

Anderson R. F. (1987) Redox behaviors of uranium in an anoxic marine basin. *Uranium* **3,** 145–164.

Anderson R. F., Bopp R. F., Buesseler K. O., and Biscaye P. E. (1988) Mixing of particles and organic constituents in sediments from the continental shelf and slope off Cape Cod: SEEP-I results. *Cont. Shelf Res.* **8,** 925–946.

Anderson R. F., Fleisher M. Q., and LeHuray A. P. (1989a) Concentration, oxidation state and particulate flux of uranium in the Black Sea. *Geochim. Cosmochim. Acta* **53,** 2215–2224.

Anderson R. F., LeHuray A. P., Fleisher M. Q., and Murray J. W. (1989b) Uranium deposition in Saanich Inlet sediments, Vancouver Island. *Geochim. Cosmochim. Acta* **53,** 2205–2213.

Anderson R. F. and Fleisher M. Q. (1991) Uranium precipitation in Black Sea sediments. In *Black Sea Oceanography* (eds. E. Izdar and J. W. Murray), pp. 443–458. Kluwer Academic Publishers.

Anderson R. F., Rowe G. T., Kemp P. F., Trumbore S., and Biscaye

P. E. (1994) Carbon budget for the mid-slope depocenter of the Middle Atlantic Bight. *Deep-Sea Res.* **41,** 669–703.

Barnes C. and Cochran J. K. (1988) The geochemistry of uranium in marine sediments. In *Radionuclides: A Tool for Oceanography* (eds. J. C. Guary, P. Guegueniat, and R. J. Pentreath), pp. 162–170. Elsevier.

Barnes C. E. and Cochran J. K. (1990) Uranium removal in oceanic sediments and the oceanic U balance. *Earth Planet. Sci. Lett.* **97,** 94–101.

Barnes C. E. and Cochran J. K. (1991) Geochemistry of uranium in Black Sea sediments. *Deep-Sea Res.* **38,** S1237–S1254.

Biscaye P. E. and Anderson R. F. (1994) Fluxes of particulate matter on the slope of the southern Middle Atlantic Bight: SEEP-II. *Deep-Sea Res.* **41,** 459–509.

Bruland K. W., Franks R. P., and Landing W. M. (1981) Southern California inner basin sediment trap calibration. *Earth Planet. Sci. Lett.* **53,** 400–408.

Cochran J. K., Carey A. E., Sholkovitz E. R., and Surprenant L. D. (1986) The geochemistry of uranium and thorium in coastal marine sediments and sediment pore water. *Geochim. Cosmochim. Acta* **50,** 663–680.

Colley S., Thomson J., and Toole J. (1989) Uranium relocations and derivation of quasi-isochrons for a turbidite/pelagic sequence in the Northeast Atlantic. *Geochim. Cosmochim. Acta* **53,** 1223–1234.

Colodner D. (1991) The marine geochemistry of rhenium, iridium and platinum. Ph.D. thesis. Woods Hole Oceanographic Institution, Massachusetts Institute of Technology.

Crusius J. and Anderson R. F. (1992) Inconsistencies in accumulation rates of Blank Sea sediments inferred from records of *Laminae* and [210]Pb. *Paleoceanography* **7,** 215–227.

Crusius J., Calvert S., Pedersen T., and Sage D. (1996) Rhenium and molybdenum enrichments in sediments as indicators of oxic, suboxic and sulfidic conditions of deposition. *Earth Planet. Sci. Lett.* **145,** 65–78.

Emery K. O. (1960) *The Sea Off Southern California.* Wiley.

Fleisher M. Q., Anderson R. F., and LeHuray A. P. (1986) Uranium deposition in ocean margin sediments. *Eos Trans. AGU* **67**, 1070.

Francois R. (1988) A study on the regulation of the concentrations of some trace metals (Rb, Sr, Zn, Pb, Cu, V, Cr, Ni, Mn and Mo) in Saanich Inlet sediments, British Columbia. *Mar. Geol.* **83**, 285–308.

Fredrickson J. K., Zachara J. M., Kennedy D. W., Duff M. C., Gorby Y. A., Li S. W., and Krupka K. M. (2000) Reduction of U(VI) in goethite (a-FeOOH) suspensions by a dissimilatory metal-reducing bacterium. *Geochim. Cosmochim. Acta* **64**, 3085–3098.

Gardner J. V., Dean W. E., and Dartnell P. (1997) Biogenic sedimentation beneath the California Current system for the past 30 kyr and its paleoceanographic significance. *Paleoceanography* **12**, 207–225.

Huh C.-A., Zahnle D. L., Small L. F., and Noshkin V. E. (1987) Budgets and behaviors of uranium and thorium series isotopes in Santa Monica Basin sediments. *Geochim. Cosmochim. Acta* **51**, 1743–1754.

Hulsemann J. and Emery K. O. (1963) Stratification in recent sediments of Santa Barbara Basin as controlled by organisms and water characteristics. *J. Geol.* **69**, 279–290.

Jahnke R. A. (1988) A simple, reliable, and inexpensive pore-water sampler. *Limnol. Oceanogr.* **33**, 483–487.

Jahnke R. A. (1990) Early diagenesis and recycling of biogenic debris at the seafloor, Santa Monica Basin, California. *J. Mar. Res.* **48**, 413–436.

Klinkhammer G. P. and Palmer M. R. (1991) Uranium in the oceans: Where it goes and why. *Geochim. Cosmochim. Acta* **55**, 1799–1806.

Kochenov A. V., Korolev K. G., Dubinchuk V. T., and Medvedev Y. L. (1977) Experimental data on the conditions of precipitation of uranium from aqueous solutions. *Geochem. Int.* **14**, 82–87.

Kolodny Y. and Kaplan I. R. (1973) Deposition of uranium in the sediment and interstitial water of an anoxic fjord. In *Proceedings of the Symposium on Hydrogeochemistry and Biogeochemistry*, Vol. 1 (ed. E. Ingerson), pp. 418–442. Clarke.

Kuwabara J. S., van Geen A., McCorkle D. C., and Bernhard J. M. (1999) Dissolve sulfide distribution in the water column and sediment porewaters of Santa Barbara Basin. *Geochim. Cosmochim. Acta* **63**, 2199–2209.

Langmuir D. (1978) Uranium solution–mineral equilibrium at low temperature with applications to sedimentary ore deposits. *Geochim. Cosmochim. Acta* **42**, 547–569.

Li Y.-H. and Gregory S. (1974) Diffusion of ions in sea water and in deep-sea sediments. *Geochim. Cosmochim. Acta* **38**, 703–714.

Liger E., Charlet L., and van Cappellen P. (1999) Surface catalysis of uranium (VI) reduction by iron (II). *Geochim. Cosmochim. Acta* **63**, 2939–2955.

Lovley D. R., Phillips E. J. P., Gorby Y. A., and Landa E. R. (1991) Microbial reduction of uranium. *Nature* **350**, 413–416.

Lovley D. R. and Phillips E. J. P. (1992) Reduction of uranium by *Desulfovibrio desulfuricans. Appl. Environ. Microbiol.* **58**, 850–856.

Lovley D. R., Roden E. E., Phillips E. J. P., and Woodward J. C. (1993) Enzymatic iron and uranium reduction by sulfate-reducing bacteria. *Mar. Geol.* **113**, 41–53.

Lyle M., Zahn R., Prahl F., Dymond J., Collier R., Pisias N., and Suess E. (1992) Paleoproductivity and carbon burial across the California Current: The multitracers transect, 42°N. *Paleoceanography* **7**, 251–272.

Martin W. R. and Sayles F. L. (1987) Seasonal cycles of particles and solute transport processes in nearshore sediments: $^{222}Rn/^{226}Ra$ and $^{234}Th/^{238}U$ disequilibrium at a site in Buzzards Bay, MA. *Geochim. Cosmochim. Acta* **51**, 927–943.

Muramoto J. A., Honjo S., Fry B., Hay B. J., Howarth R. W., and Cisne J. L. (1991) Sulfur, iron and organic carbon fluxes in the Black Sea: Sulfur isotopic evidence for origin of sulfur fluxes. *Deep-Sea Res.* **38(Suppl. 2)**, S1151–S1187.

Murray J. W., Jannasch H. W., Honjo S., Anderson R. F., Reeburgh W. S., Top A., Friederich G. E., Codispoti L. A., and Izdar E. (1989) Unexpected change in the oxic/anoxic interface in the Black Sea. *Nature* **338**, 411–413.

Næs K., Skei J. M., and Wassmann P. (1988) Total particulate and organic fluxes in anoxic Framvaren waters. *Mar. Chem.* **23**, 257–268.

Nameroff T. J. (1996) Suboxic trace metal geochemistry and paleorecord in continental margin sediments of the eastern tropical North Pacific. Ph.D. thesis. University of Washington.

Reimers C. E., Jahnke R. A., and McCorkle D. C. (1992) Carbon fluxes and burial rates over the continental slope and rise off central California with implications for the global carbon cycle. *Global Biogeochem. Cycles* **6**, 199–224.

Reimers C. E., Ruttenberg K. C., Canfield D. E., Christiansen M. B., and Martin J. B. (1996) Porewater pH and authigenic phases formed in the uppermost sediments of the Santa Barbara Basin. *Geochim. Cosmochim. Acta* **60**, 4037–4057.

Scranton M. I., Sayles F. L., Bacon M. P., and Brewer P. G. (1987) Temporal changes in the hydrography and chemistry of the Cariaco Trench. *Deep-Sea Res.* **34**, 945–963.

Shaw T. J., Gieskes J. M., and Jahnke R. J. (1990) Early diagenesis in differing depositional environments: The response of transition metals in pore water. *Geochim. Cosmochim. Acta* **54**, 1233–1246.

Sholkovitz E. R. (1973) Interstitial water chemistry of the Santa Barbara Basin sediments. *Geochim. Cosmochim. Acta* **37**, 2043–2073.

Sholkovitz E. R. and Gieskes J. M. (1971) A physical-chemical study of the flushing of the Santa Barbara Basin. *Limnol. Oceanogr.* **16**, 479–489.

Sirocko F., Sarnthein M., Lange H., and Erlenkeuser H. (1991) Atmospheric summer circulation and coastal upwelling in the Arabian Sea during the Holocene and the last glaciation. *Quat. Res.* **36**, 72–93.

Skei J. M., Loring D. H., and Rantala R. T. T. (1988) Partitioning and enrichment of trace metals in a sediment core from Framvaren, South Norway. *Mar. Chem.* **23**, 269–281.

Taylor S. R. and McLennan S. M. (1985) *The Continental Crust: Its Composition and Evolution.* Blackwell.

Thomson J., Higgs N. C., Wilson T. R. S., Croudace, L. W., de Lange G. J., and van Santvoort P. J. M. (1995) Redistribution and geochemical behavior of redox-sensitive elements around S1, the most recent eastern Mediterranean sapropel. *Geochim. Cosmochim. Acta* **59**, 3487–3501.

Thunell R. C., Tappa E., and Anderson D. M. (1995) Sediment fluxes and varve formation in Santa Barbara Basin. *Geology* **23**, 1083–1086.

Todd J. F., Elsinger R. J., and Moore W. S. (1988) The distribution of uranium, radium and thorium isotopes in two anoxic fjords; Framvaren Fjord (Norway) and Saanich Inlet (Br. Columbia). *Mar. Chem.* **23**, 393–415.

Toole J., Thomson J., Wilson T. R. S., and Baxter M. S. (1984) A sampling artifact affecting the uranium content of deep-sea porewaters obtained from cores. *Nature* **308**, 263–266.

Toole J., McKay K., and Baxter M. (1991) Determination of uranium in marine sediment pore waters by isotope dilution inductively coupled plasma mass spectrometry. *Anal. Chim. Acta* **245**, 83–88.

Wallace H. E., Thomson J., Wilson T. R., Weaver P. P. E., Higgs N. C., and Hydes D. J. (1988) Active diagenetic formation of metal-rich layers in N. E. Atlantic sediments. *Geochim. Cosmochim. Acta* **52**, 1557–1569.

Wheatcroft R. A., Jumars P. A., Smith C. R., and Nowell A. R. M. (1990) A mechanistic view of the particulate biodiffusion coefficient: Step lengths, rest periods and transport directions. *J. Mar. Res.* **48**, 177–207.

Zheng Y. (1999) The marine geochemistry of germanium, molybdenum and uranium: The sinks. Ph.D. thesis. Columbia University.

Zheng Y., Anderson R. F., van Geen A., and Kuwabara J. (2000) Authigenic molybdenum formation in marine sediments: A link to pore water sulfide in the Santa Barbara Basin. *Geochim. Cosmochim Acta* **64**, 4165–4178.

Zheng Y. Anderson R. F., van Geen A., and Fleisher, M. Q. (2002) Preservation of particulate non-lithogenic uranium in marine sediments. *Geochim. Cosmochim Acta* **66**, in press.